Structure and Phonon Investigations of an Extended Family of Lithium (Thio)Boracite Electrolytes for All-Solid-State Batteries

D. Cory Lynch [I], and N. A. W. Holzwarth [I]
[I] Department of Physics, Wake Forest University, Winston-Salem, NC 27109, USA

Introduction

Previous experimental and computational investigations into the (thio) boracite family of materials have shown promisingly high ionic conductivities within stable framework structures, which has motivated the computational investigation of an extended family of (thio) boracite materials presented in this work. In addition to the three compositions based on published literature, $Li_4B_7O_{12}Cl$ [1,2], $Li_4Al_3B_4O_{12}Cl$ [3,4], and $Li_6B_7S_{13}I$ [5], we have included five newly predicted compositions for a total of eight (thio) boracite materials to investigate: $Li_4B_7O_{12}Cl$, $Li_4Al_3B_4O_{12}Cl$, $Li_4B_7S_{12}Cl$, $Li_4Al_3B_4S_{12}Cl$, $Li_6B_7O_{13}Cl$, $Li_6Al_3B_4O_{13}Cl$, $Li_6B_7S_{13}Cl$, and $Li_6Al_3B_4S_{13}Cl$. In our collection of materials, we have chosen to look at $Li_6B_7S_{13}Cl$ instead of the experimentally observed $Li_6B_7S_{13}I$ so that we have a consistent halogen choice. The five newly predicted materials are based on the material differences (sulfur-oxygen substitution; different Li stoichiometries). In this work, we present structural investigations and phonon analysis of all eight (thio) boracite materials.

Calculational Methods

Structural relaxation calculations were performed using QUANTUM ESPRESSO [6] and ABINIT [7] software packages, based on density functional theory (DFT) [8]. These DFT calculations were done using the PBESol [9] exchange correlation functional. The Projector Augmented Wave (PAW) [10] formalism was used, and the basis and projector functions were generated by the ATOMPAW [11] code. The total electronic energy determined from DFT structural relaxation approximates the static lattice internal energy of the system denoted by $U_{SL}(\{N_i\})$.

Phonon calculations were performed using the Finite Differences [12] method as implemented in the PHONOPY [13] software package. Optimal band paths were calculated using the SEEKPATH [14] software. With the static lattice and vibrational energies found, we can then approximate the Helmholtz free energy as follows:

$$F(T,V,\{N_i\}) \approx U_{SL}(\{N_i\}) + F_{vib}(T,V,\{N_i\})$$

Structural Investigations

Previous experimental and computational works involving $Li_4B_7O_{12}Cl$ gave the starting point of our investigations. The disordered F-43c structure of the Li_4 boracite was found to relax into a low energy ordered R3c structure, where the partially occupied Li sites map into a fully occupied Li configuration. The remaining "empty" sites from the cubic setting carry over as rhombohedral interstitial sites for the Li to naturally diffuse through. Similar ordered R3c structures were found for the remaining seven materials investigated. All the Li_4 materials except $Li_4B_7S_{12}Cl$ have the space group R3c as their lowest energy structures, as does $Li_6B_7O_{13}Cl$. In Table 1, we summarize structural information based on $U_{SL}(\{N_i\})$ calculations.

Table 1 (left): Conventional cell structural information for the eight (thio) boracite materials in different space group configurations, where "SG" details the space group, "Lattice" details the lattice parameters in Angstroms, "Angle" details the lattice angles in degrees, "Tri/Tet" details the framework ratio of BO_3/BS_3 triangular planar to BO_4/BS_4 tetrahedral structural units, "Vol" details the cell volume per formula unit in cubic Angstroms, and "ΔU_{SL}" details the static lattice energies referenced to the Li_4 R3c static lattice energy (defined to be zero energy). The values in parenthesis indicate the experimental values, where a refers to reference 1, b to reference 3, and c to reference 5.

Formula	SG	Lattice	Angle	Tri/Tet	Vol	ΔU_{SL}
$Li_4B_7O_{12}Cl$	*R3c*	a =12.1 (12.1410)[a]	α =90.1 (90.0)[a]	4/3	223.0	0.00
$Li_4B_7O_{12}Cl$	*F43c*	a =12.2	α =90.0	4/3	224.8	0.21
$Li_6B_7O_{13}Cl$	*R3c*	a =12.2	α =89.4	1/6	224.3	-1.58
$Li_6B_7O_{13}Cl$	*Cc*	a =15.0	α =90.0	1/6	225.8	-1.26
		b = 8.6	β =124.7			
		c = 8.6	γ =90.0			
$Li_4Al_3B_4O_{12}Cl$	*R3c*	a =13.0 (12.9687)[b]	α =91.1 (90.0)[b]	4/3	275.6	0.00
$Li_4Al_3B_4O_{12}Cl$	*F43c*	a =13.0	α =90.0	4/3	272.0	1.19
$Li_6Al_3B_4O_{13}Cl$	*R3c*	a =13.0	α =88.3	1/6	275.0	-0.22
$Li_6Al_3B_4O_{13}Cl$	*Cc*	a =16.0	α =90.0	1/6	273.8	-0.40
		b = 8.9	β =127.1			
		c = 9.7	γ =90.0			
$Li_4B_7S_{12}Cl$	*R3c*	a =14.9	α =89.8	4/3	415.7	0.00
$Li_4B_7S_{12}Cl$	*F43c*	a =14.9	α =90.0	4/3	414.6	-0.05
$Li_6B_7S_{13}Cl$	*R3c*	a =15.1 (15.245)[c]	α =89.2 (90.0)[c]	0/7	431.3	-0.96
$Li_6B_7S_{13}Cl$	*Cc*	a =18.5	α =90.0	0/7	429.9	-1.05
		b =10.5	β =124.6			
		c =10.8	γ =90.0			
$Li_4Al_3B_4S_{12}Cl$	*R3c*	a =16.1	α =89.6	4/3	516.9	0.00
$Li_4Al_3B_4S_{12}Cl$	*F43c*	a =15.8	α =90.0	4/3	489.0	0.85
$Li_6Al_3B_4S_{13}Cl$	*R3c*	a =16.1	α =87.8	0/7	519.7	-0.34
$Li_6Al_3B_4S_{13}Cl$	*Cc*	a =19.8	α =90.0	0/7	508.2	-0.65
		b =10.8	β =126.1			
		c =11.8	γ =90.0			

Table 2 (below): Calculated Helmholtz free energies for selected configurations of the eight (thio) boracite materials. "SG" represents the space group, and "ΔF" columns represents the Helmholtz free energy referenced to the Li_4 R3c configuration. The Helmholtz free energy has been calculated at three temperatures: 0K, 300K, and 400K.

Formula	SG	ΔF T =0K	ΔF T =300K	ΔF T =400K
$Li_4B_7O_{12}Cl$	*R3c*	0.00	0.00	0.00
$Li_6B_7O_{13}Cl$	*R3c*	-1.59	-1.53	-1.50
$Li_6B_7O_{13}Cl$	*Cc*	-1.27	-1.22	-1.20
$Li_4Al_3B_4O_{12}Cl$	*R3c*	0.00	0.00	0.00
$Li_6Al_3B_4O_{13}Cl$	*R3c*	-0.25	-0.20	-0.18
$Li_6Al_3B_4O_{13}Cl$	*Cc*	-0.42	-0.35	-0.32
$Li_4B_7S_{12}Cl$	*R3c*	0.00	0.00	0.00
$Li_4B_7S_{12}Cl$	*F43c*	-0.07	-0.09	-0.10
$Li_6B_7S_{13}Cl$	*R3c*	-0.96	-0.92	-0.89
$Li_6B_7S_{13}Cl$	*Cc*	-1.05	-0.99	-0.96
$Li_4Al_3B_4S_{12}Cl$	*R3c*	0.00	0.00	0.00
$Li_6Al_3B_4S_{13}Cl$	*R3c*	-0.33	-0.23	-0.19
$Li_6Al_3B_4S_{13}Cl$	*Cc*	-0.63	-0.52	-0.47

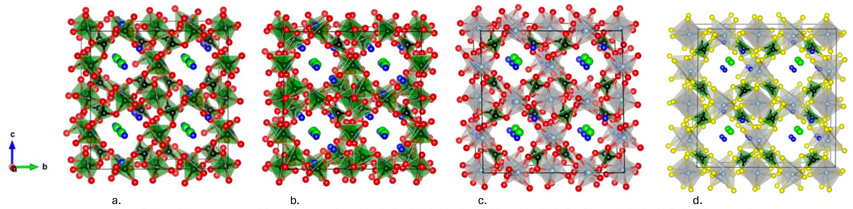

Relaxed lowest energy R3c structures for a.) $Li_4B_7O_{12}Cl$, b.) $Li_6B_7O_{13}Cl$, c.) $Li_4Al_3B_4O_{12}Cl$, and d.) $Li_4Al_3B_4S_{12}Cl$ materials

In addition to the ordered R3c structure, an ordered cubic F-43c can be determined by selecting specific Wyckoff positions for the lithium, but in most cases, this is energetically prohibitive. Only $Li_4B_7S_{12}Cl$ has this as its lowest energy phase.

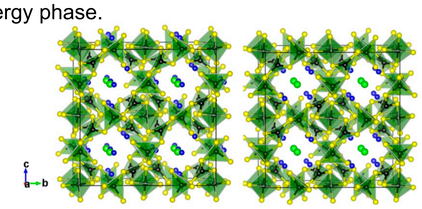

Relaxed a.) higher energy R3c $Li_4B_7S_{12}Cl$ and b.) lowest energy F-43c $Li_4B_7S_{12}Cl$ structures.

Atomic Species Color Key (Structure and PDOS Plots)

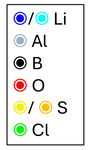

Interestingly, the $Li_6B_7S_{13}I$ was reported to have a lower energy tetrahedral phase. Investigating this structure for $Li_6B_7S_{13}Cl$ led to the discovery of an even lower energy Cc structure for this material. This was done by optimizing structures found during first principles molecular dynamics simulations. Similar Cc structures were also found for all eight materials in the study. For all Li_6 materials except $Li_6B_7O_{13}Cl$, this is the lowest energy structure of the three space groups investigated.

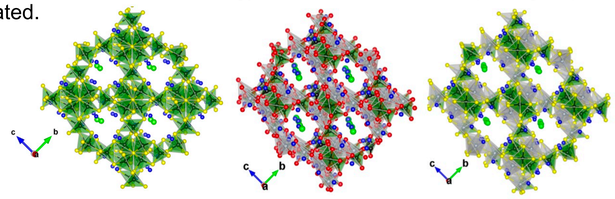

Relaxed lowest energy Cc structures for a.) $Li_6B_7S_{13}Cl$, b.) $Li_6Al_3B_4O_{13}Cl$, and c.) $Li_6Al_3B_4S_{13}Cl$

Phonon Analysis

Phonon calculations were performed on all eight materials' lowest energy structures – calculating the phonon bands, partial density of phonon states, and the vibrational contributions to the Helmholtz free energy (Table 2). We find some very interesting details when analyzing the partial density of phonon states. The Cl modes have a very narrow range of frequencies near 100 cm^{-1}. The Li atoms occupy the void regions of the crystals and are coupled to framework modes. They vibrate within a broad range of frequencies from roughly 100 to 400 cm^{-1}. The mid and high frequency range contains the localized vibrations of the framework structural units only, involving either BO_3/BS_3 or BO_4/BS_4. The highest frequency bands are the vibrations involving only the triangular BO_3/BS_3 units. The Al modes found at the mid range frequencies are associated with AlO_4/AlS_4 structural units. Al is not found at the higher frequencies as there are no AlO_3/AlS_3 structural units.

Band and PDOS Plots for Lowest Energy Structures (below):
The plots below each contain two subplots. The subplot on the left contains the band structure plot for the material along the optimal band path provided by SEEKPATH[14] (along the x-axis), with frequencies measured in cm^{-1} (along the y-axis). The subplot on the right depicts phonon density of states for each of the chemical species (along the x-axis) vs the phonon frequency in cm^{-1} (along the y-axis). See the Color Key provided for the species color representations.

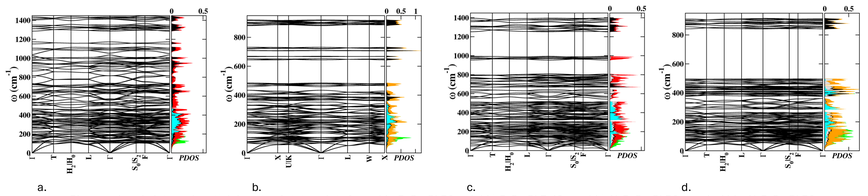

Phonons band plots and partial density of states plots for a.) $Li_4B_7O_{12}Cl$ R3c, b.) $Li_6B_7S_{12}Cl$ F-43c, c.) $Li_4Al_3B_4O_{12}Cl$ R3c, and d.) $Li_4Al_3B_4S_{12}Cl$ R3c

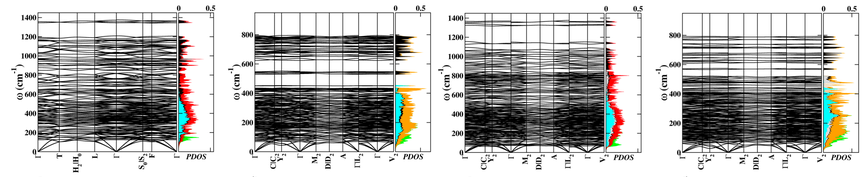

Phonons band plots and partial density of states plots for a.) $Li_6B_7O_{13}Cl$ R3c, b.) $Li_6B_7S_{13}Cl$ Cc, c.) $Li_6Al_3B_4O_{13}Cl$ Cc, and d.) $Li_6Al_3B_4S_{13}Cl$ Cc

Conclusions

In this work, we have investigated an extended family of eight (thio) boracite materials based on three experimentally studied materials: $Li_4B_7O_{12}Cl$, $Li_4Al_3B_4O_{12}Cl$, and $Li_6B_7S_{13}I$. We have expanded upon previous structural knowledge, extending the previously determined lowest energy R3c structural ordering of $Li_4B_7O_{12}Cl$ to the other materials. We have found that this is also the lowest energy structure for $Li_4Al_3B_4O_{12}Cl$, $Li_4Al_3B_4S_{12}Cl$, and $Li_6B_7O_{13}Cl$. We have also determined lower energy structures for the remaining materials: F-43c for $Li_4B_7S_{12}Cl$, and Cc for $Li_6B_7S_{13}Cl$, $Li_6Al_3B_4O_{13}Cl$, and $Li_6Al_3B_4S_{13}Cl$.

Phonon calculations were performed, allowing us to investigate the vibrational modes of the framework as well as the Li and Cl ions located in the void regions of the materials. These calculations also allowed us to determine the vibrational contributions to the Helmholtz free energy at 0K, 300K, and 400K for the lowest energy structures of each material, as well as selected higher energy configurations (Table 2). The Helmholtz free energies allow us to assess whether the inclusion of thermal vibrational energies affect the energetic ordering of the materials' structures. When we add the vibrational energies to the static lattice energies to calculate the Helmholtz free energy, the pattern seen in Table 1 does not change.

Not presented here, but included in our preprint [15], we utilize methods based on static lattice energies for assessing the stability of these materials, including Convex Hull and Voltage Window analyses. Future work is planned to assess ionic conductivity and analyze ion migration mechanisms in these materials.

Acknowledgments

We would like to acknowledge NSF grants DMR-1940324 and DMR- 2242959 for financial support, WFU High Performance Computing Facility for compute resources and technical support, and co-authors Yan Li [II] and Pieremanuele Canepa [II, III, IV].
[II] Department of Materials Science and Engineering, National University of Singapore, Singapore, 119077
[III] Department of Electrical and Computer Engineering, University of Houston, Houston, Texas 77204, USA
[IV] Texas Center for Superconductivity at the University of Houston (TcSUH), Houston, Texas 77204, USA

References

1. W. Jeitschko, et. al. "Crystal Structure and Ionic Conductivity of Li Boracites." DOI: 10.1107/S0567740877009443
2. Y. Li, et. al. "First-Principles Simulations of Li Boracites $Li_4B_7O_{12}Cl$ and $Li_3B_7O_{12.5}Cl$." DOI: 10.1103/PhysRevMaterials.6.025401
3. K. Kajihara, et. al. "$Li_6B_4MO_{13}Cl$ (M = Al, Ga): An Electrochemically Stable, Lithium-Ion-Conducting Cubic Boracite ..." DOI: 10.1007/978-981-33-6668-8_21
4. D. Tan, et. al. "Low-Temperature Ionothermal Synthesis of Li-Ion Conductive $Li_4B_7O_{12}Cl$ Solid-State Electrolyte." DOI: 10.1021/acsaem.9b00812
5. K. Kaup, et. al. "Fast Ion-Conducting Thioboracite with a Perovskite Topology and Argyrodite-like Lithium Substructure." DOI: 10.1021/jacs.1c00941
6. P. Giannozzi, et. al. "Quantum espresso toward the exascale." DOI: 10.48550/arXiv.2104.10502
7. X. Gonze, et al. "Recent developments in the ABINIT software package." DOI: 10.1016/j.cpc.2016.04.003
8. P. Hohenberg, et. al. "Inhomogeneous electron gas." DOI: 10.1103/PhysRev.136.B864
9. J. P. Perdew, et. al. "Restoring the Density-Gradient Expansion for Exchange in Solids and Surfaces." DOI: 10.1103/PhysRevLett.100.136406
10. P. E. Blochl. "Projector augmented-wave method." DOI: 10.1103/PhysRevB.50.17953
11. N. A. W. Holzwarth, et. al. "A Projector Augmented Wave (PAW) code for electronic structure calculations ..." DOI: 10.1016/S0010-4655(00)00244-7
12. L. Chaput, et. al. "Phonon-phonon interactions in transition metals." DOI: 10.1103/PhysRevB.84.094302
13. A. Togo. "First-principles phonon calculations with phonopy and phono3py." DOI: 10.7566/JPSJ.92.012001
14. Y. Hinuma, et al. "Band structure diagram paths based on crystallography." DOI: 10.1016/j.commatsci.2016.10.015
15. D. C. Lynch, et. al. "Computational investigation of the structural and electrolyte properties of the extended family ...". (Preprint)